

Shadow Detection and Removal in Video Sequence using Color-Based Method

Dr. Zainab M. Hussain

Al-Mansour University College

Informatics Institute For Postgraduate Studies

zainab_hussain2012@yahoo.com

Ali Ataemah Jebur

M.Sc Student

ali.taima@yahoo.com

Abstract

Moving shadow elimination is an important step in many applications of computer vision such as tracking, surveillance system, traffic monitoring etc. In this paper, a new method which combining two color spaces (HSV and YCbCr) with background modelling will be proposed to detect and remove cast shadow. The proposed shadow detection and removal method is implemented in indoor and outdoor with humans, vehicles, and motorcycles moving objects in different times and environments including various weather and lighting conditions, such as periods of sun, sunset, rainy, noisy, and darkness and different light sources. The results shows that the proposed system gives a high performance measures as compared with another shadow detection methods and its able to cope with different environments.

Keywords: *Shadow Detection, Color Space, Background Modelling.*

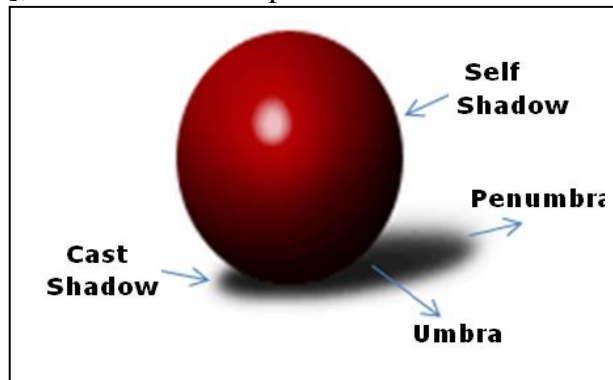
الخلاصة

أزاله الظل المتحرك هي خطوة مهمة في العديد من تطبيقات رؤية الحاسوب كالتتبع، أنظمة المراقبة، مراقبة المرور، الخ. في هذا البحث طريقة جديدة التي تمزج فضائي لون (HSV and YCbCr) مع نمذجة الخلفية سوف يتم اقتراحهما لكشف وحذف الظل الساقط. طريقة كشف وحذف الظل المقترحة تم تطبيقها داخلياً وخارجياً مع البشر، المركبات، والدراجات النارية في أوقات وبيئات تتضمن مختلف ظروف الإنارة والطقس كالشمس، الغروب، المطر، العتمة ومختلف مصادر الضوء. النتائج بينت أن النظام المقترح أعطى مقياس أداء عالي مقارنة بطرق كشف ظل أخرى وقدرته على التعامل مع مختلف البيئات.

1. Introduction

Many computer vision applications dealing with video require detecting and tracking moving objects. When the objects of interest have a well defined shape, template matching or more sophisticated classifiers can be used to directly segment the objects from the image. These techniques work well for well defined objects such as vehicles but are difficult to implement for non-rigid objects such as human bodies. However, current techniques typically have one major disadvantage: shadows tend to be classified as part of the foreground. This happens because shadows share the same movement patterns and have a similar magnitude of intensity change as that of the foreground objects.

Shadows and shadings in images occur when objects occlude light from a light source and they appear as surface features. In general, shadows can be divided into two major classes: Self shadow and Cast shadow. Figure(1)[1]; shows some examples of different kinds of shadows in images.



Cast shadows can be further divided into umbra and penumbra region, which is a result of multi-lighting and self-shadows also have many sub-regions such as shading and anti reflection. Usually, the self-shadow are not clearshadows and do not have clear boundaries. On the other hand, cast shadows are hard shadows and always have a rigid contrast to background. Because of these different properties, algorithms to process these two kinds of shadows are dissimilar. For example, algorithms to handel shadows cast by buildings and vehicles in traffic systems could not deal with the shadows on a human face.

In the real world, shadows can be generally divided into static shadow and dynamic shadow. Static shadows are cast by static object such as buildings, trees, parked cars etc. Dynamic shadows in video are cast by moving objects such as moving vehicles the penumbra is the region in which only a portion of the light source is obscured by the occluding body. The umbra is the darkest part of the shadow in the umbra; the light source is completely occluded [2].

Since cast shadows can be as big as the actual objects, their incorrect classification as foreground results in inaccurate detection, and decreasestracking performance. Example scenarios where detection and tracking performance are affected include: (i) several people are merged together because of their cast shadows, (ii) the inclusion of shadow pixels decreases the reliability of the appearance model for each person, increasing the likelihood of tracking loss[3,4].

In this paper study the features of shadow in various color models and proposed a new hybrid system combining two color spaces (HSV and YCbCr) with a background modelling to detect and remove moving cast shadow.

The organization of this paper is as follows: In section 2, The background modelling was explained. Section 3 reviews the shadow detection techneques. Section 4 describes the shadow detection methodologies. Section 5 explain the performance mesures of the shadow detection method. Section 6 present the proposed shadow detection and removal system. Finally, Section 7 present the experimental results of the proposed system and conclusions of this study are given in section 8.

2- Background Modeling

Foreground identifies pixel in the video frame that cannot be adequately explained by the background model, and output them as a binary candidate foreground mask. There are many methods to deal with background modeling in video sequence. The approximated Median Filter (AMF) model is a simple adaptive single mode background model that it stores information regarding one mode of the background image's pixel values. The method was developed due to the success of median filtering on a buffer of images. Let x_t denote the current sample value and let m_t denote the current approximation of the median, $m_t + 1$ is then approximated by

$$m_t + 1 = \begin{cases} m_t + \alpha & \text{if } X_t > m_t \\ m_t - \alpha & \text{if } X_t < m_t \\ m_t & \text{if } X_t = m_t \end{cases} \dots \dots \dots (1)$$

where α is set depending on the desired rate of convergence[5].

3-Shadow Detection Techniques

Shadow detection is applied to locate the shadow regions and distinguish shadows from foreground objects. There are many techniques based on shadow properties to detect shadow [1,3]:-

A- Model Based technique:-In this technique, the 3D geometry and illumination of the scene are assumed to be known. This includes the sensor/camera localization, the light source direction, and the geometry of observed objects, from which a priori knowledge of shadow areas is derived [1].

B- Image based technique:- This makes use of certain image shadow properties such as color (or intensity), shadow structure (umbra and penumbra hypothesis), boundaries, etc., without any

assumption about the scene structure. Nevertheless, if any of that information is available, it can be used to improve the detection process performance.

C- Color /spectrum technique: - The color model technique attempts to describe the color change of shaded pixel and find the color feature that is illumination invariant. Cucchiara, investigated the Hue-Saturation-Value (HSV) color property of cast shadows, and it is found that shadows change the hue component slightly and decrease the saturation component significantly. The shadow pixels cluster in a small region that has distinct distribution compared with foreground pixels. The shadows are then discriminated from foreground objects by using empirical thresholds on HSV color spac. Salvador *et al*, proposed anormalized RGB color space, C1C2C3, to segment the shadows in still images and video sequences[1]. K. Siala, consider the pixel’s intensity change equally in RGB color components and a diagonal model is proposed to describe the color distortion of shadow in RGB space[3].

D- Texture technique: -The principle behind the textural technique is that the texture of foreground objects is different from that of the background, while the texture of shaded area remains the same as that of the background. The several techniques have been developed to detect moving cast shadows in a normal indoor environment. [1,3].

E-Geometry techniques: - Geometric technique makes use of the camera location, the ground surface, and the object geometry, etc., to detect the moving cast shadows. Gaussian shadow model was proposed to detect the shadows of pedestrian. The model is parameterized with several features including the orientation,mean intensity, and center position of a shadow region with the orientation and centroid position being estimated from the properties of object moments[1,3].

4- Shadow Detection Methodologies

Shadow detection is applied to locate the shadow regions and distinguish shadows from foreground objects. There are many approaches based on shadow properties to detect shadow [1]:-

4.1 Explanation of color based techneques

These techneques based on the color change of shaded pixel and find the color features that is illumination invariant.Some of these methods are:

4.1.1- Hue, Saturation, Value- HSV

The Hue, Saturation, Value- HSV color space separates color into three components, hue, saturation, and value. It was introduced and developed for use in computer graphics to specify color in way more closely related to how the humans perceive color then when specified in terms of red, green, and blue.Conversion to HSV from RGB is done by the following equations [5]:

$$V = \max(R, G, B) \dots \dots \dots (2)$$

$$S = \begin{cases} \frac{\max(R, G, B) - \min(R, G, B)}{\max(R, G, B)} & \text{if } \max(R, G, B) \neq 0 \dots \dots \dots (3) \\ 0 & \text{otherwise} \end{cases}$$

$$H = \begin{cases} \frac{G - B}{\max(R, G, B) - \min(R, G, B)} & \text{if } R = \max(R, G, B), \\ 2 + \frac{B - R}{\max(R, G, B) - \min(R, G, B)} & \text{if } G = \max(R, G, B) \dots \dots \dots (4) \\ 4 + \frac{R - G}{\max(R, G, B) - \min(R, G, B)} & \text{if } B = \max(R, G, B). \end{cases}$$

For image and video processing applications there are some drawbacks using HSV.The hue for values close to the achromatic axis will be more or less unstable depending on the noise introduced by the capturing device. Also, both the saturation and hue components will be unreliable in dark regions due low signal to noise ratio.

4.1.2.Improved Hue, Saturation, Lightness – IHSL

Noting the drawbacks of the HSV and other similar color spaces for image processing applications an alternative 3D-polar color representation was presented. As with HSV, the color is described using the three components, hue, saturation, and lightness. Lightness, or lightness function, is in this case a more general term for value. The saturation is independent of the lightness function used and the hue is defined as in HSV. Conversion to IHSL from RGB as the lightness function is done by the following equations [1,5,6]:-

$$Y = 0.2126R + 0.7152G + 0.0722B \dots\dots\dots (5)$$

$$S = \max(R, G, B) - \min(R, G, B) \dots\dots\dots (6)$$

$$H = \begin{cases} 2\pi - \arccos\left(\frac{R - G/2 - B/2}{\sqrt{R^2 + G^2 + B^2 - RG - RB - BG}}\right) & \text{if } B > G \\ \arccos\left(\frac{R - G/2 - B/2}{\sqrt{R^2 + G^2 + B^2 - RG - RB - BG}}\right) & \text{otherwise} \end{cases} \dots\dots\dots (7)$$

One advantage is that a better suited lightness function can be used, the value V used in HSV conflicts badly with our perception of lightness. However, as with any color space defining a hue as above, it suffers from it being undefined for RGB-values on the achromatic axis.

4.1.3.YC_bC_rColor Space

The YC_bC_r color space separates color into a luminance component and two chromaticity components. The main reason for the existence of the YC_bC_r color space is a historical one, when color TVs were introduced there was a need to be backwards compatible with black and white TVs, and the separation of luminance and chrominance made this possible. The human visual system is far less sensitive to errors in chromaticity than luminance; allowing for less bandwidth to be used to transmit the chromaticity information. It is still used today because of this, along with the fact that conversion to and from RGB is very simple. Conversion to YC_bC_r is done via YPbPr which denotes YC_bC_r prior to offset and scaling for digital storage. The following transformation is used to convert gamma corrected 3 ITU Rec. 709 RGB-values $\hat{R}, \hat{G}, \hat{B}$ to $\hat{Y}pbpr$ -values using [5]:

$$\hat{Y} = 0.2126\hat{R} + 0.7152\hat{G} + 0.0722\hat{B} \dots\dots\dots (8)$$

$$Pb = 0.25389(\hat{B} - \hat{Y}) \dots\dots\dots (9)$$

$$Pr = 0.6350(\hat{R} - \hat{Y}) \dots\dots\dots (10)$$

where $\hat{Y} \in [0, 1]$, $Pb \in [-0.5, 0.5]$, and $Pr \in [-0.5, 0.5]$, and the gamma correction is done using[5]:

$$\hat{R} = 1.099R^{0.45} - 0.099 \dots\dots\dots (11)$$

$$\hat{G} = 1.099G^{0.45} - 0.099 \dots\dots\dots (12)$$

$$\hat{B} = 1.099B^{0.45} - 0.099 \dots\dots\dots (13)$$

The color spaces HSV and IHSL are compared using the same hypothesis, which is that a shadowed pixel value's value and saturation will decrease while the hue remains relatively constant.

Let x_f, x_b denote a foreground and background pixel value respectively, they can be RGB-vectors, HSV-vectors, or something else depending on the context. Also, let sp denote a shadow mask of the same size as the images. The hypothesis is tested by evaluating sp [1,5,6]:

$$sp = \begin{cases} 1 & \text{if } \alpha \leq \frac{x_f, L}{x_b, L} \leq \beta \\ & \wedge x_f, s - x_b, s \leq TS \\ & \wedge |x_f, h - x_b, h| \leq TH \\ 0 & \text{otherwise} \end{cases} \dots\dots\dots (14)$$

where L denotes the lightness function and is V for HSV and Y for IHS. α, β, TS, TH are thresholds. Y'PbPr can be compared in a similar manner under the hypothesis that the lightness or luminance component should decrease and the chromaticity coordinates should remain relatively constant. Using the same notation as above, sp can be expressed as

$$sp = \begin{cases} 1 & \text{if } \alpha \leq \frac{x_{f,L}}{x_{b,L}} \leq \beta \\ & \wedge (x_{f,c1} - x_{b,c1})^2 + (x_{f,c2} - x_{b,c2})^2 \leq TC \dots\dots\dots(15) \\ 0 & \text{otherwise} \end{cases}$$

where L denotes the lightness function and is \hat{Y} for \hat{Y} PbPr, and c1, c2 denotes the chromaticity coordinates and Pb, Pr for \hat{Y} PbPr. α, β, TC are thresholds [5].

4.2.Normalized Difference Index-NDI

The input image which is denoted by I is first converted to HSV color space using the following equations[7]:

$$V = \frac{1}{3}(R + G + B) \dots\dots\dots(16)$$

$$S = 1 - \frac{3}{R + G + B} \min(R, G, B) \dots\dots\dots(17)$$

$$H = \begin{cases} \theta & \text{if } B \leq G \\ 360^\circ - \theta & \text{if } B > G \end{cases} \dots\dots\dots(18)$$

In which

$$\theta = \cos^{-1} \left\{ \frac{\frac{1}{2}[(R - G) + (R - B)]}{\sqrt{(R - G)^2 + (R - B)(G - B)}} \right\} \dots\dots\dots(19)$$

It has been observed that shadow areas are dark and saturated strongly with the blue and violet wavelength. In HSV color space, shadows hold some different spectral properties as follows:

- 1) low value because the direct light from the Sun is occluded by elevated objects;
- 2) high saturation with short blue-violet wavelength due to atmospheric Rayleigh scattering effect;
- 3) high hue values because shadow areas are dark.

Hue is an attribute associated with the dominant wavelength in a mixture of light waves. Hue represents dominant color as perceived by an observer. Saturation refers to the relative purity or the amount of white light mixed with hue. Thus, shadow areas have maximum value of saturation and the minimum value component in HSV color space. Some other features like vegetation, roads etc. have similar characteristics. The S and V components of I are used to extract shadows using Normalized Difference Index NDI as,[7]:

$$NDI = \frac{S - V}{S + V} \dots\dots\dots(20)$$

In order to detect shadow areas, a positive threshold T can be found to segment the NDI images.

$$I_{shadow}(i, j) = \begin{cases} 1 & NDI(i, j) \geq T \\ 0 & NDI(i, j) \leq T \end{cases} \dots\dots\dots(21)$$

4.3.Photometric Color Invariants

A spectral property of shadows can be derived in the commented hypothesis by considering photometric color invariants. Photometric color invariants are functions which describe the color configuration of each image point discounting shading, shadows, and highlights. These functions are demonstrated to be invariant to a change in the imaging conditions, such as viewing

direction, object's surface orientation and illumination conditions. Let us define F as one of the above mentioned photometric color invariants[8].

$$F1 = Fs \dots \dots \dots (22)$$

F1 is the value assumed in a point in light, and Fs is the value in the same point in shadow. Then, Examples of photometric color invariants are normalized rgb, hue (H), saturation (S), c1c2c3 and l1l2l3. In particular, among the different photometric invariant color features, the c1c2c3 model has been tested. The c1c2c3 invariant color features are defined as follows[8]:

$$c1(x, y) = \arctan \frac{R(x, y)}{\max(G(x, y), B(x, y))} \dots \dots \dots (23)$$

$$c2(x, y) = \arctan \frac{G(x, y)}{\max(R(x, y), B(x, y))} \dots \dots \dots (24)$$

$$c3(x, y) = \arctan \frac{B(x, y)}{\max(R(x, y), G(x, y))} \dots \dots \dots (25)$$

for R(x, y), G(x, y) and B(x, y) representing the red, green, and blue color components of a pixel in the image.

4.4.Division Based Brightness Invariants:

Another way to achieve invariant parameters is to normalize the RGB values to the intensity factor. This can be done by division of color signals. Examples of this type of parameters are normalized RGB (r g b), saturation calculated by the following equation [8]:

$$s = \frac{\max\{R, G, B\} - \min\{R, G, B\}}{\max\{R, G, B\}} \dots \dots \dots (26)$$

or the new introduced colors like c1c2c3 mentioned above and l1l2l3:

$$l1 = \frac{(R - G)^2}{(R - G)^2 + (R - B)^2 + (G - B)^2} \dots \dots \dots (27)$$

$$l2 = \frac{(R - B)^2}{(R - G)^2 + (R - B)^2 + (G - B)^2} \dots \dots \dots (28)$$

$$l3 = \frac{(G - B)^2}{(R - G)^2 + (R - B)^2 + (G - B)^2} \dots \dots \dots (29)$$

which are suggested by Gever[8]. Yet another brightness invariant model can be obtained by calculation:

$$r1 = \frac{\max\{G, B\} - R}{\max(R, G, B)} \dots \dots \dots (30)$$

$$r2 = \frac{\max\{R, B\} - G}{\max(R, G, B)} \dots \dots \dots (31)$$

$$r3 = \frac{\max\{R, G\} - B}{\max(R, G, B)} \dots \dots \dots (32)$$

It is shown that in some forest road scenes, segmentation by r3 yields to better results in comparison to other brightness invariant parameters.

4.5. Textures Based Shadow Removal

Some methods exploit the fact that regions under shadow retain most of their texture. Texture-based shadow detection methods typically follow two steps:

1. selection of candidate shadow pixels or regions, and
2. classification of the candidate pixels or regions as either foreground or shadow based on texture correlation.

Selection of the shadow candidates is done with a weak shadow detector, usually based on spectral features. Then, each shadow candidate is classified as either object or shadow by correlating the texture in the frame with the texture in the background reference. If a candidate's texture is similar in both the frame and the background, it is classified as shadow. Various methods perform this correlation with various techniques (e.g. normalized cross-correlation, gradient or edge correlation, orthogonal transforms, Markov or conditional random fields, Gabor filtering)[3]. Texture correlation is a potentially powerful method for detecting shadows as textures are highly distinctive, do not depend on colors, and are robust to illumination changes

Normalized cross correlation (NCC) can be useful to detect shadow pixel candidates, since it can identify scaled versions of the same signal. Let $B(i, j)$ be the background image, and $I(i, j)$ be an image of the video sequence. For each pixel (i, j) belonging to the foreground, consider a $(2N + 1) \times (2N + 1)$ template T_{ij} such that $T_{ij}(n,m) = I(i+n, j+m)$, for $-N \leq n \leq N, -N \leq m \leq N$ (i.e. T_{ij} corresponds to a neighborhood of pixel (i,j)) Then, the NCC between template T_{ij} and image B at pixel (i, j) is given by [4]:

$$NCC(i, j) = \frac{ER(i, j)}{E_B(i, j)E_{T_{ij}}}, \dots \dots \dots (33)$$

Where

$$ER(i, j) = \sum_{n=-N}^N \sum_{m=-N}^N B(i + n, j + m)T_{ij}(n, m), \dots \dots \dots (34)$$

$$E_B(i, j) = \sqrt{\sum_{n=-N}^N \sum_{m=-N}^N B(i + n, j + m)^2}, \dots \dots \dots (35)$$

$$E_{T_{ij}} = \sqrt{\sum_{n=-N}^N \sum_{m=-N}^N T_{ij}(n, m)^2} \dots \dots \dots (36)$$

For a pixel (i, j) in a shadowed region, the NCC in a neighboring region T_{ij} should be larger (close to one), and the energy $E_{T_{ij}}$ of this region should be lower than the energy $E_B(i, j)$ of the corresponding region in the background image. Thus, a pixel (i, j) is pre-classified as shadow if :

$$NCC(i, j) \geq L_{NCC} \text{ and } E_{T_{ij}} < E_B(i, j) \dots \dots \dots (37)$$

Where L_{NCC} is a fixed threshold. If L_{NCC} is low, several foreground pixels corresponding to moving objects may be misclassified as shadow. On the other hand, selecting a larger value for L_{NCC} results in less false positives, but pixels related to actual shadows may not be detected.

4.6.Shadow Removal by LaplacianEdge Detection

Among many types of edge detection methods such as Canny and Sobel, the Laplacian edgedetector with kernel 3×3 of figure(2) will be choosed to reduce computation costs and also ensure a good result in common conditions.

Let $L_{CF}(x, y)$ and $L_{BG}(x, y)$ denoted the outcome results of convolution of laplacian kernel with a pixel at (x, y) in the blob regions of the current frame, and with a pixel at (x, y) in the corresponding region of the background, respectively.

-1	-1	-1
-1	8	-1
-1	-1	-1

Figure.2 Laplacian Kernel.

During convolution of the laplacian kernel, if the neighbor pixel of the pixel at (x, y) doesn't belong to blob regions in the foreground mask, we ignore it (take the gray-level intensity of the neighbor pixel as 0). Now the $Diff(x, y)$ is define as [9]:

$$Diff(x, y) = L_{BG}(x, y) * L_{CF}(x, y) \dots \dots \dots (38)$$

If for a pixel at (x, y) in the foreground mask,

$$Diff(x, y) \geq 0 \dots \dots \dots (39)$$

Then the pixel at (x, y) is considered as a shadow region pixel.

However, there exist situations where even if the formula (38) is satisfied, the pixel at (x, y) in the foreground mask may not be a shadow region pixel but an object blob pixel. This can often happen in the situation with a complex background. But practically there are some reason why we believe this rule is still acceptable in general situations.

4.7.Shadow Detection in Gradient

The moving object could be removed as shadows if can only use the property based on color, if the gradient can be accepted, the foreground can be detected more effectively. In a video surveillance system, vehicles and people always have abundant texture information. Similar to the color-based shadow removal method, a texture distortion measure can detect possible foreground shadow pixels [10].

The gradient density difference and the related gradient score can be computed using [6]:

$$GD_i(x, y) = GD_{I,i}(x, y) - GD_{B,i}(x, y) \dots \dots \dots (40)$$

$$S_{G,i}(x, y) = \begin{cases} 1 & GD_i(x, y) \leq T_{G1} \\ \frac{[T_{G2} - GD_i(x, y)]}{T_{G2} - T_{G1}} & T_{G1} < GD_i(x, y) < T_{G2} \dots \dots \dots (41) \\ 0 & GD_i(x, y) \geq T_{G2} \end{cases}$$

$GD_i(x, y)$ is the gradient density difference between the i^{th} input image and the i^{th} background image at location (x, y) . Here, T_{G1} and T_{G2} are two predefined thresholds and $GD_{I,i}(x, y)$ and $GD_{B,i}(x, y)$ are the average of gradient magnitudes over a spatial window are in the masked input frame and corresponding masked background at pixel (x, y) . The gradient density values are mostly cancelled out in the cast shadow region and pixel with small gradient difference value is more likely to be a part of the cast shadow region.

5. Performance Measure

The performance of any shadow detection and removal system can be tested using two metrics proposed by Prati et al [11], namely shadow detection rate (η) and shadow discrimination rate (ξ):

$$\eta = \frac{TP_S}{TP_S + FN_S} \dots \dots \dots (42)$$

$$\xi = \frac{TP_F}{TP_F + FN_F} \dots\dots\dots (43)$$

Where TP and FN stand for true positive and false negative pixels with respect to either shadows(S) or foreground objects (F). The shadow detection rate is concerned with labelling the maximum number of cast shadow pixels as shadows. The shadow discrimination rate is concerned with maintaining the pixels that belong to the moving object as foreground.

6. The Proposed Method

In this paper a shadow detection and removal system was proposed based on the hybrid of two color spaces (HSV and YCbCr) with a background modelling. The structure diagram of the proposed system is illustrated in figure (3). The video is generated using a static webcam which captured to grip RGB image at a specific time. The background model will be generated and updated at each capturing process using AMF algorithm. The current image will go to the shadow detection and removal algorithm which based on the new proposed hybrid color model (HSV and YCbCr), the output of this process is an RGB image without shadow.

6.1. Capture Process

This process is performed using “WebCam_Capture.dll” visual basic 2008 library which is capturing the frame from webcam by setting its properties:

“CaptureHeight” and CaptureWidth” to set the height and width of the captured frames. The size of the captured frames are set to (250X250). The property “TimeToCapture_milliseconds” is used to set the time of capturing process in milliseconds with (5fps). Finally the frame capturing is holds in picture box tool which available on the visual basic.

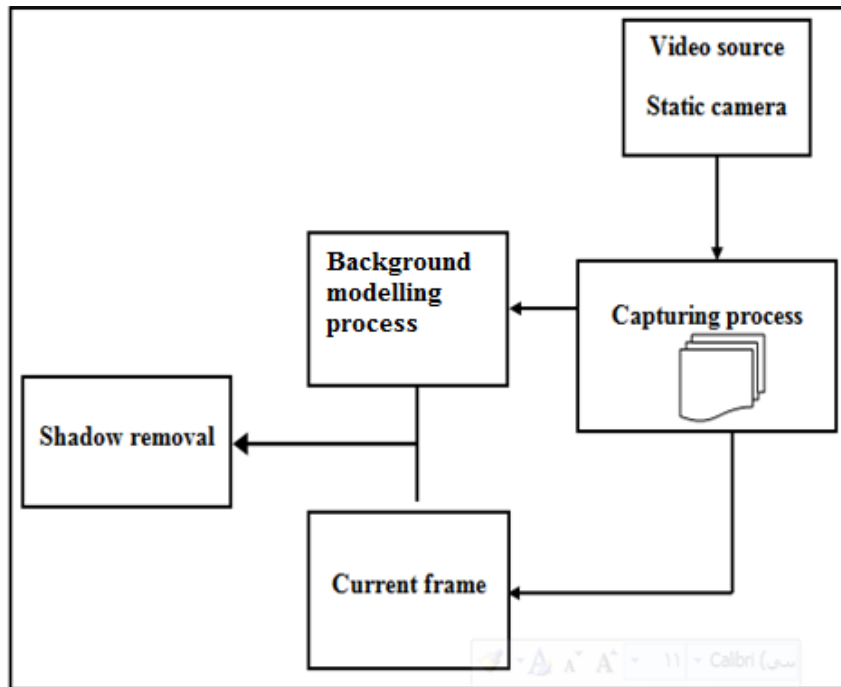


Figure. 3. Block diagram for the proposed shadow detection and removal system

6.2. Background Modeling Process

Using the AMF model the first frame of the video sequence can be used as an initial guess or it can be simply set to 0. To use this algorithm on multi-dimensional frames, for example (RGB) color, assuming each color channel or dimension is independent, the median can be estimated separately for each dimension. The background model can be modeled using equation (1).

Using the notations in table (1) the core of the pseudo code of the Approximate Median Filtering algorithm can be written as shown in algorithm (1).

Table (1). Notations for algorithm 1.(Approximate Median Filtering)

Symbols	Meaning
X	Frame height
Y	Frame width
FR	Red channel in current frame
FG	Green channel in current frame
FB	Blue channel in current frame
BGR	Red channel in BG
BGG	Red channel in BG
BGB	Red channel in BG
α	Adaptation rate

<p>Algorithm 2 Approximate Median Filtering Input:RGB Image Output:RGB Image(represent background model) 1: set first frame as BG . 2: for X=0 to height-1 do 3: for Y=0 to width-1 do 4: if FR > BGR then 5: BGR = BGR + α 6: if FR < BGR then 7: BGR = BGR - α 8: else 9: BGR=BGR 10:end if 11:if FG>BGG then</p>	<p>12: BGG=BGG + α 13: else if FG < BGG then 14: BGG=BGG - α 15: else 16: BGG=BGG 17: endif 18: if FB>BGB then 19: BGB=BGB + α 20: else if FB < BGB then 21: BGB=BGB - α 22: else 23: BGB=BGB 22: end if 23: end for Y 24: end for X</p>
--	---

6.3. Shadow Removal Process

It is the core of the shadow detection and removal system. In this system a hybrid method combining two color spaces (HSV and YC_bC_r) was proposed this method work without any assumption about the scene structure such as camera localization, the light source direction, and the geometry of observed objects and work very fast so its suitable to implement on imbedded system and for real time applications.

First of all the RGB images can be converted to HSV color space using the equations (2,3,4) and to YC_bC_r color space using the equations(8,9,10). After that the cast shadow pixels can be determined using the equations (14,15) and finally the pixel $I(x, y)$ can be classified as shadow or foreground using the following proposed criteria:-

$$I(x, y) = \begin{cases} Shadow & \text{if } sp1 = 1 \text{ and } sp2 = 1 \\ Foreground & \text{otherwise} \end{cases} \dots \dots \dots (44)$$

Where sp1 and sp2 represent shadow detection in HSV and YC_bC_r respectively.Using the notations in table (2) the core of the shadow detection and removal algorithm can be written in pseudo code as shown in algorithm (2).

Table 2 Notations for algorithm 2(shadow detection and removal)

Symbols	Meaning	Symbols	Meaning
X	Frame height	BG _H	Hue for BG
Y	Frame width	F _y	Y channel for current image
FR	Red channel in current frame	F _{Cb}	Cb channel for current image
FG	Green channel in current frame	F _{Cr}	Cr channel for current image
FB	Blue channel in current frame	BG _y	Y channel for BG
BG _R	Red channel in BG	BG _{Cb}	Cb channel for BG
BG _G	Green channel in BG	BG _{Cr}	Cr channel for BG
BG _B	Blue channel in BG	Sp1	HSV Binary image
Result _R	Red channel in current image without the shadow	Sp2	YCbCr Binary image
Result _G	Green channel in current image without the shadow	T _{v1} , T _{v2}	Value (intensity) minimum Threshold , Value (intensity) maximum Threshold
Result _B	Blue channel in current image without the shadow	T _s	Saturation Threshold
F _v	Value (intensity) for current frame	T _H	Hue Threshold
F _s	Saturation for current frame	T _{y1} , T _{y2}	Y minimum Threshold, Y maximum Threshold
F _H	Hue for current frame	T _{Cb1} , T _{Cb2}	Cb minimum Threshold, Cb maximum Threshold
BG _v	Value (intensity) for BG	T _{Cr1} , T _{Cr2}	Cr minimum Threshold, Cr maximum Threshold
BG _s	Saturation for BG		

<p>Algorithm 2 shadow detection and removal. Input:Two RGB images(current image & background model) Output:RGB image(without shadow) 1: for X=0 to height-1 do 2: for Y=0 to width-1 do 3: Calculat F_v, F_s, F_H,BG_v,BG_s,BG_H 4: Calculat F_y, F_{Cb}, F_{Cr},BG_y,BG_{Cb},BG_{Cr} 5: If (F_v / BG_v ≥ T_{v1} And F_v / BG_v ≤ T_{v2}) And (F_s - BG_s) ≤ T_s And F_H - BG_H ≤ T_H Then 6: sp1 = 1 7: Else 8: sp1 = 0 9: End If</p>	<p>10: If (F_y / BG_y ≥ T_{y1} And F_y / BG_y ≤ T_{y2}) And (F_{Cb} - BG_{Cb} ≥ T_{Cb1} And F_{Cb} - BG_{Cb} ≤ T_{Cb1}) And (F_{Cr} - BG_{Cr} ≥ T_{Cr1} And F_{Cr} - BG_{Cr} ≤ T_{Cr1}) Then 11: Sp2 = 1 12: Else 13: Sp2 = 0 14: End If 15: If Sp1=1 and Sp2=1 then 16: result_R=BG_R 17: result_G=BG_G 18: result_B=BG_B 19: Else 20: result_R=FR 21: result_G=FG 22: result_B=FB 23: Endif 24: end for Y 25: endfor X</p>
--	--

7-Experimental Results

The practical implementation and evaluation of the proposed shadow detection and removal system is discussed in this section. The system is implemented indoor and outdoor with humans, and vehicles in different times. These tested images sequences included various weather and

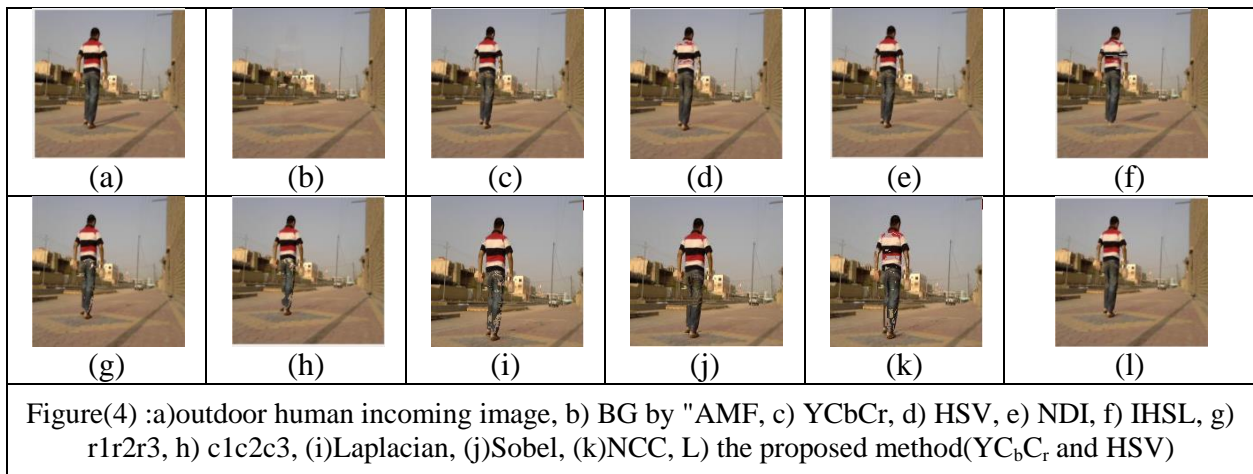
lighting conditions, including periods of sun and darkness and different light sources. The proposed shadow detection method (HSV and YC_bC_r) was tested using three situations of indoor walked human, outdoor walked human and outdoor vehicle. Then it compared with another nine shadow detection methods (HSV, IHSL, YC_bC_r , NDI, c1c2c3, r1r2r3, Laplacian, Gradient, NCC) which were designed and implemented. This comparison was done using the two evaluation measures shadow detection rate (η) and shadow discrimination rate (ξ) equations (42 and 43).

7-1 Situations

- **First Situation** (outdoor walked human) in sunny day with large cast shadow region. Table (3) shows the setting parameters for all the shadow detection methods. Figure (4) illustrates the results of applying all these shadow detection methods on the outdoor image.

Table (3) Parameters setting.(outdoor walked human)

Methods	Parameters
HSV	$\alpha = 0.7 , \beta = 1 , TS = 1 , TH = 2$
IHSL	$\alpha = -10 , \beta = 30 , TS = 30 , TH = 30$
YC_bC_r	$\alpha = 0.4 , \beta = 1 , -40 \leq Tc \leq 40$
NDI	$1 \leq T \leq 1.5$
c1c2c3	$Tc1 = 0.05 , Tc2 = 0.05 , Tc3 = 0.05$
r1r2r3	$-0.1 \leq Tr1 \leq 0.1 , -0.1 \leq Tr2 \leq 1 , -0.1 \leq Tr3 \leq 0.1$
Laplacian	$Diff(x, y) \geq -45 , Diff(x, y) \leq 45$
Gradient	$T_{G1} \leq 0 , T_{G2} \geq 1.5$
NCC	$L_{NCC} \geq 0.995$
HSV& YC_bC_r	$\alpha = 0.7 , \beta = 1 , TS = 1 , TH = 2 , -40 \leq Tc \leq 40$



From this figure it can be seen that the proposed method gives the most accurate image than the other methods. Table (4) shows the quantities for shadow detection rate and shadow discrimination rate for all tested methods to the above outdoor human scene, and figure (6) shows the chart for this quantities, using three bars for each tested method, blue for shadow detection rate, red for shadow discrimination rate, and green for the average for this two rates.

Table (4) Shadow detection rate and Shadow discrimination rate.(outdoor human scene)

Methods	Shadow Detection Rate	Shadow Discrimination Rate	Average
NDI	0.5075885	0.8137321	0.6606603
YCbCr	0.5996649	0.8868116	0.7432383
IHSL	0.4085213	0.8963290	0.6524251
C1C2C3	0.4568764	0.8905506	0.6737135
r1r2r3	0.1893491	0.8861318	0.537740498
NCC	0.3402985	0.8789938	0.6096461
Laplacian	0.4156305	0.8589394	0.6372850
Gradient	0.4697247	0.7675050	0.6186149
HSV	0.4333925	0.7583276	0.5958601
HSV&YCbCr	0.6342412	0.8857919	0.7600166

The above results illustrate that the proposed method(HSV and YCbCr) gives the higher shadow detection rate and shadow discrimination rate, consequently it gives higher average of the two rates.

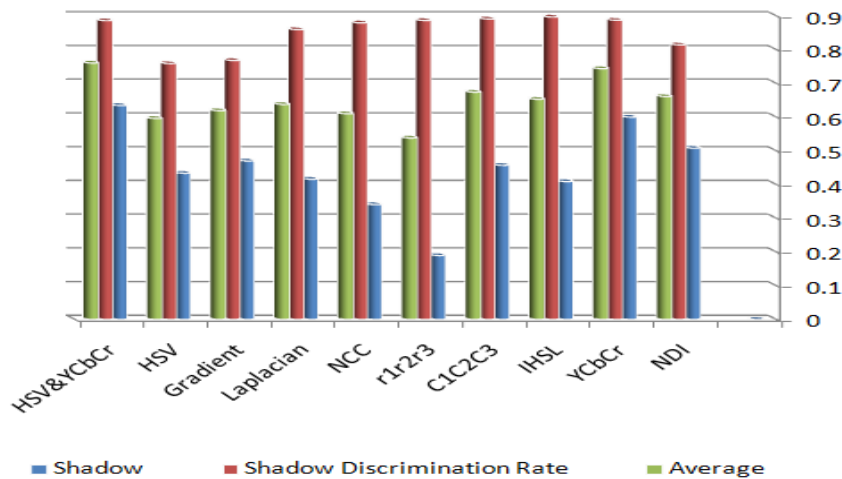


Figure 5 chart for table(4) out door human

• **Second Situation** (outdoor vehicle) in sunset time with low light condition. Table(5) shows the setting parameters for all the shadow detection methods. Figure(6) illustrates the results of applying all these shadow detection methods on the outdoor vehicle image.

Table 5 Parameter settings.(outdoor vehicle)

Methods	Parameters
HSV	$\alpha = 0.3, \beta = 1, TS = 1, TH = 2$
IHSL	$\alpha = -10, \beta = 30, TS = 100, TH = 100$
YCbCr	$\alpha = 0.5, \beta = 1, -40 \leq Tc \leq 40$
NDI	$1 \leq T \leq 2.5$
c1c2c3	$Tc1 = 0.04, Tc2 = 0.04, Tc3 = 0.04$
r1r2r3	$-0.3 \leq Tr1 \leq 0.5, -0.3 \leq Tr2 \leq 5, -0.3 \leq Tr3 \leq 0.5$
Laplacian	$Diff(x, y) \geq -45, Diff(x, y) \leq 45$
Gradient	$T_{G1} \leq 0, T_{G2} \geq 1.5$
NCC	$L_{NCC} \geq 0.9$
HSV&YCbCr	$\alpha = 0.3, \beta = 1, TS = 1, TH = 2, -40 \leq Tc \leq 40$

From this figure it can be seen that the proposed method gives a good accurate image compared with the other methods. Table (6) shows the quantities for shadow detection rate and shadow discrimination rate for all the tested methods to the outdoor vehicle scene, and figure (7) shows the chart for these quantities, using three bars for each tested method, blue for shadow detection rate, red for shadow discrimination rate, and green for the average for this two rates.

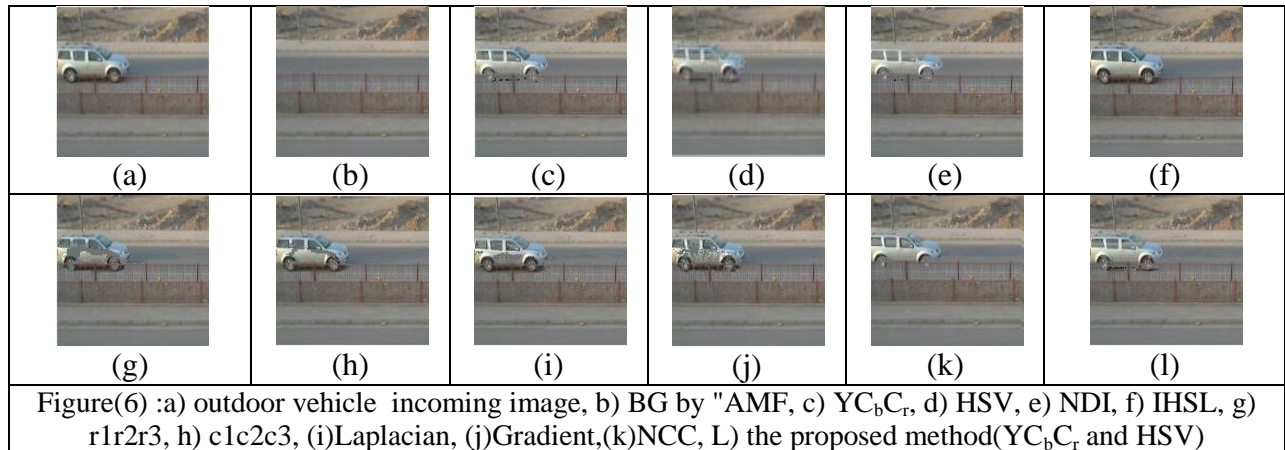
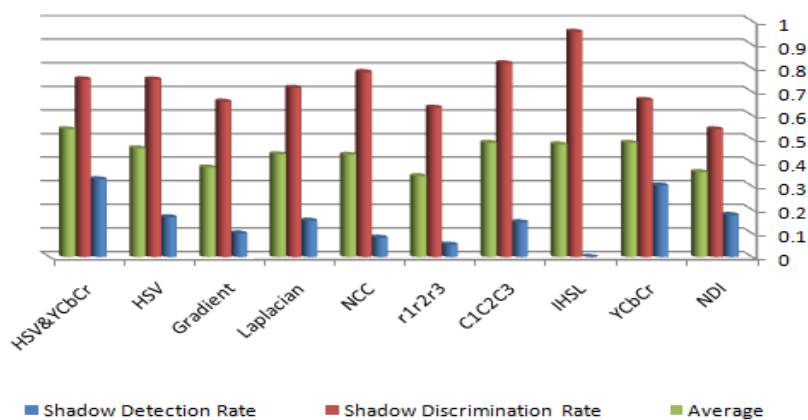


Table (6) Shadow detection rate and Shadow discrimination rate.(outdoor human scene)

Methods	Shadow Detection Rate	Shadow Discrimination Rate	Average
NDI	0.178519594	0.541533546	0.36002657
$YCbCr$	0.302839117	0.666134185	0.484486651
IHSL	0	0.955271565	0.477635783
C1C2C3	0.147540984	0.821618743	0.484579863
r1r2r3	0.052711994	0.633120341	0.342916167
NCC	0.082278481	0.784345048	0.433311764
Laplacian	0.154566745	0.717784878	0.436175811
Gradient	0.100250627	0.659211928	0.379731277
HSV	0.16893733	0.752928647	0.460932989
HSV& $YCbCr$	0.330039526	0.753461129	0.541750327



Figure(7) chart for table(6) outdoor vehicle

The results illustrates that the proposed method (HSV and YCbCr) gives an acceptable shadow detection rate and shadow discrimination rate, consequently it gives an acceptable average of the two rates.

- **Third Situation**(indoor walked humane) in room with white light sources. Table(7) shows the setting parameters for each one of the shadow detection methods. Figure(8) illustrates the results of applying all these shadow detection methods on indoor walked humane image. From this figure it can be seen that the proposed method gives the most accurate image than the other methods.

Table 7. Parameter settings. (indoor walked humane)

Methods	Parameters
HSV	$\alpha = 0.6 , \beta = 1 , TS = 1, TH = 2$
IHSL	$\alpha = -10 , \beta = 30 , TS = 100, TH = 100$
YCbCr	$\alpha = 0.6 , \beta = 1 , -40 \leq Tc \leq 40$
NDI	$1 \leq T \leq 1.5$
c1c2c3	$Tc1 = 0.05 , Tc2 = 0.05 , Tc3 = 0.05$
r1r2r3	$-0.3 \leq Tr1 \leq 0.5 , -0.3 \leq Tr1 \leq 5 ,$ $-0.3 \leq Tr1 \leq 0.5$
Laplacian	$Diff(x, y) \geq -45 , Diff(x, y) \leq 45$
Gradient	$T_{G1} \leq 0 , T_{G2} \geq 1.3$
NCC	$L_{NCC} \geq 0.999$
HSV&YCbCr	$\alpha = 0.7 , \beta = 1 , TS = 1, TH = 2,$ $\alpha = 0.7 , \beta = 1 , -20 \leq Tc \leq 40$

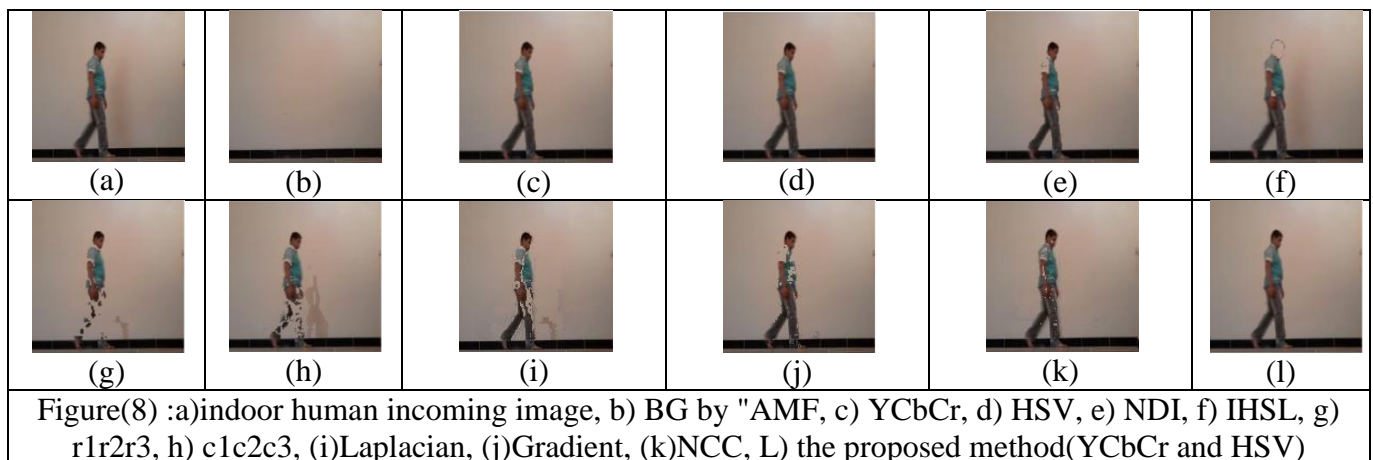
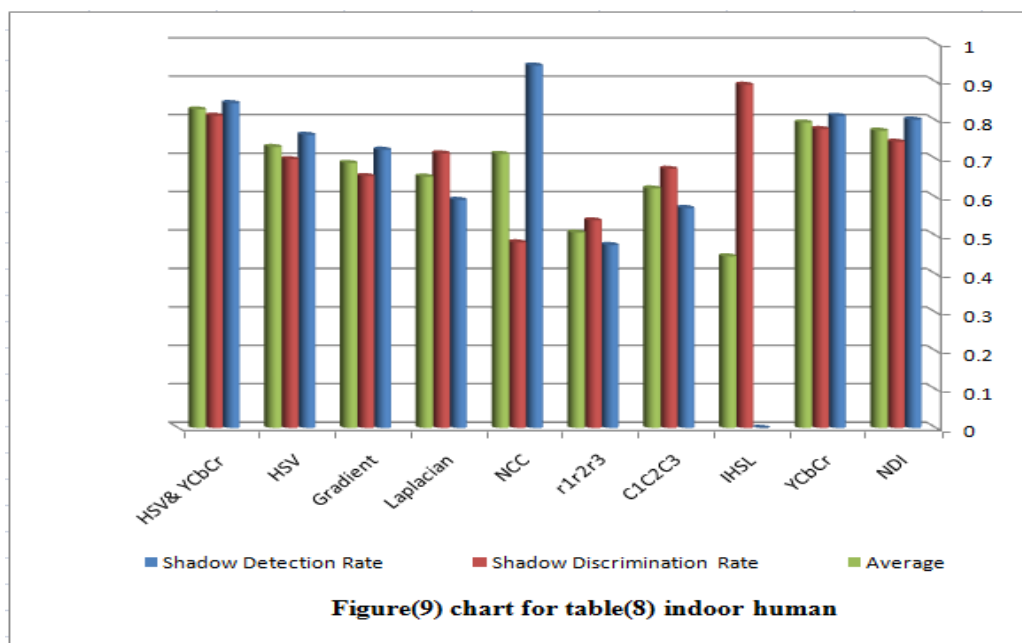


Table (8) shows the quantities for shadow detection rate and shadow discrimination rate for all tested method to the indoor walked human scene, and figure (9) shows the chart for this quantities, using three bars for each tested method, blue for shadow detection rate, red for shadow discrimination rate, and green for the average for this two rates.

Table 8.Shadow detection rate and Shadow discrimination rate. (indoor walked humane)

Methods	Shadow Detection Rate	Shadow Discrimination Rate	Average
NDI	0.802051282	0.744349573	0.773200428
YCbCr	0.811454638	0.777498744	0.794476691
IHSL	0	0.892516323	0.446258162
C1C2C3	0.571966843	0.674033149	0.622999996
r1r2r3	0.475787335	0.539929684	0.507858509
NCC	0.942461763	0.482672024	0.712566893
Laplacian	0.593175853	0.714213963	0.653694908
Gradient	0.723594325	0.654947263	0.689270794
HSV	0.762370854	0.699146158	0.730758506
HSV& YCbCr	0.844973545	0.812154696	0.828564121



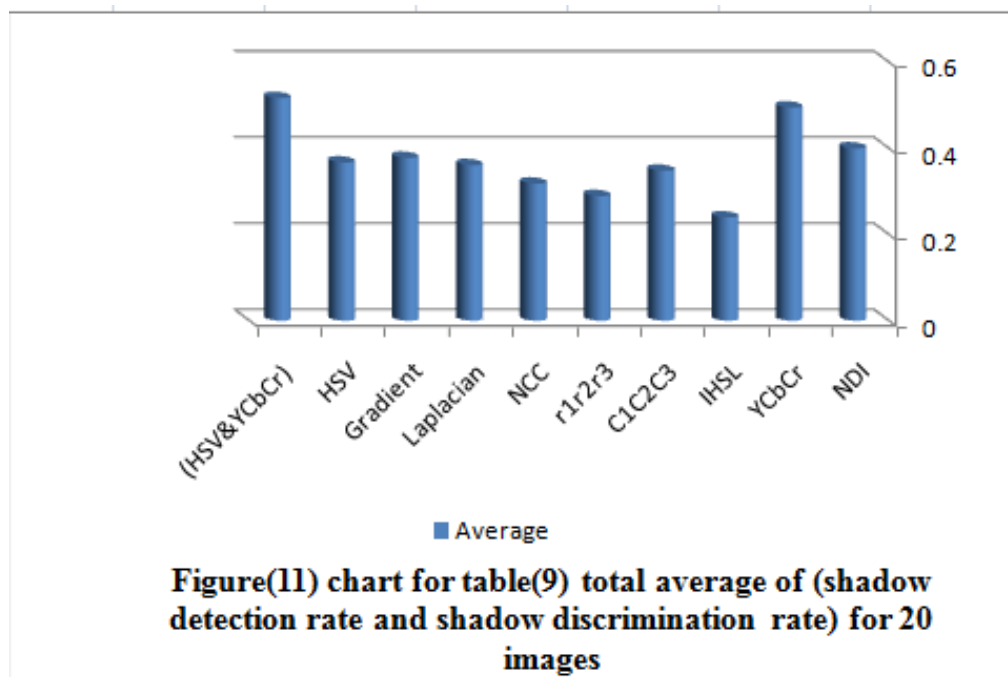
The results illustrate that the proposed method (HSV and YCbCr) gives the higher shadow detection rate and shadow discrimination rate, consequently it gives the higher average of the two rates.

20 indoor and outdoor images will be tested using the proposed system and compared with other methods. Table (9) shows the quantities of the total average of (shadow detection rate and shadow discrimination rate) for all tested methods for the 20 tested images.figure (11) shows the chart for this quantities, using one bar for each tested method.

From table (9) and figure (10) it can be seen that the proposed method (HSV and YCbCr) gives the highest values of the performance measures such that it is able to cope with different environments, light conditions such as sunny day, sunset day ,and darkness and in different light source such as sun, white , and yellow light.

Table 9 total average of (shadow detection rate and shadow discrimination rate)

Method	Average
NDI	0.400134131
YCbCr	0.495054082
IHSL	0.239665128
C1C2C3	0.348244492
r1r2r3	0.289366152
NCC	0.318294941
Laplacian	0.361134002
Gradient	0.378214208
HSV	0.367331071
(HSV&YCbCr)	0.517013927

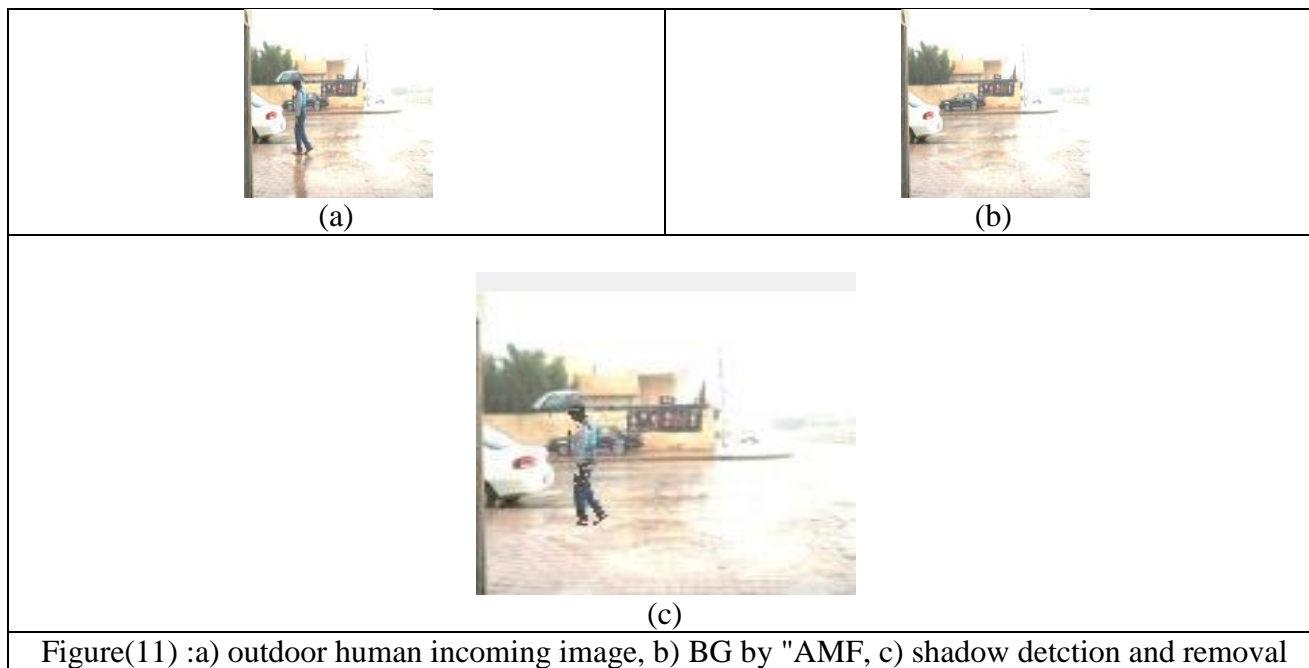


7-2 Effects of Rain on the Proposed System

To ensure the stability of the proposed system, it can be tested under natural phenomena a rainy day where the light condition is less and appear rain drop in the scene. Table (10) shows the setting parameters for the proposed algorithm to be tested under rain drop condition. Figure (11) illustrates the result of applying this system on outdoor image for human under rain drop.

Table 10. Parameter settings. (rain drop condition)

Method	Parameter
HSV	$\alpha = 0.5, \beta = 1, TS = 1, TH = 2$
&YCbCr	$\alpha = 0.5, \beta = 1, -20 \leq Tc \leq 40$



The result shows the ability of this system to detect and remove the cast shadow without be affected in rain drop.

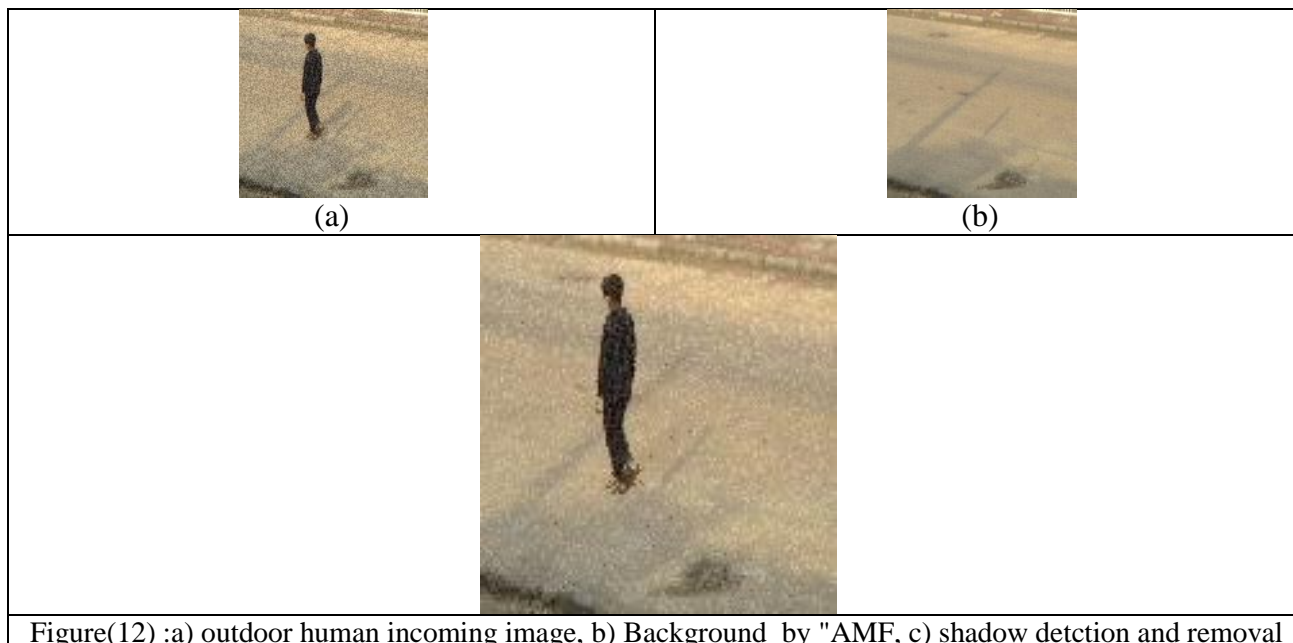
7-3 Effects of Noise on the Detection Process

To ensure the robust of the proposed algorithm it can be tested under Additive noise by adding noise to each pixel randomly with amount rang for (0) to (50). Table (11) shows the setting parameters for the proposed algorithm.

Figure (12) illustrates the result of applying the proposed system on the outdoor image for human under additive noise.

Table (11) parameter setting (Noise condition)

Method	Parameter
HSV	$\alpha = 0.7, \beta = 1, TS = 1, TH = 2$
&YCbCr	$\alpha = 0.7, \beta = 1, -20 \leq Tc \leq 40$



Form this figure it can be seen that the robust of the proposed system to remove the shadow even with the noisy environment.

8-Conclusions

In the previous sections, shadow detection and removal system using hybrid algorithms was established and its performance was tested. Various tests were performed to study the effect of various environments on performance.

The aim of this work is to improve shadow detection and removal based on hybrid methods. In the following points some remarks relating to the behavior and performance of the proposed system are incident and some derived conclusions are presented too:

1. The results show that the proposed algorithm is stable under different situations in indoor and outdoor with humans, vehicles, and motorcycles objects in different times including various weather and lighting conditions, such as periods of sun, sunset, rainy, noisy ,and darkness and different light source.
2. Shadow removal give less activity when deal with vehicles, and this don't limit the usability of the system because the small amount of cast shadow which remain from the total cast shadow don't effect on the activity of system in many application such as tracking and video surveillance.
3. The background generation using AMF is suitable for any environment and it is work without need for buffering. Also it is enable the proposed system to update the background model at each new incoming frame.

References

- [1] Kumar S.,Kaur A., "Algorithm for Shadow Detection In real Color Images",*(IJCSE) International Journal on Computer Science and Engineering* Vol. 02, No. 07, 2010.
- [2] Li G., Qin L., Huang Q., "Adaptive Moving Cast Shadow Detection", University of Chinese,2010.
- [3] Andres Sanin, Conrad Sanderson, Brian C. Lovell," Shadow detection: A survey and comparative evaluation of recent methods", The University of Queensland, School of ITEE, QLD 4072, Australia, ELSEVIER,2011.
- [4] Cezar J., Rosito C., RauppS., "Background Subtraction and Shadow Detection in Grayscale Video Sequences", University of Vale do Rio dos Sinos, 2005.
- [5] Wood J., "Statistical Background Models with Shadow Detection for Video Based Tracking", Linköpings universitet,2007.
- [6] Golzadeh S., "Shadow Aware Object Detection and Vehicle Identification via License Plate Recognition", MS.C Institute of Graduate Studies and Research, Eastern Mediterranean University,2009.
- [7] Kant K., Pal K., Nigam M., "Shadow Detection and Removal from Remote Sensing Images Using NDI and Morphological Operators", *International Journal of Computer Applications* (0975 – 8887) Volume 42– No.10, March 2012.
- [8] Junaedur M., "Motion Detection for Video Surveillance", Master Thesis Högskolan Dalarna University, 2008.
- [9] EUN B., Binh T., Tae S.,"An Efficient Cast Shadow Removal for Motion Segmentation", *Proceedings of the 9th WSEAS International Conference on Signal Processing, Computational Geometry and Artificial Vision*,2006.
- [10] Grest D., Frahm J., and Koch R., " A Color Similarity Measure for Robust Shadow Removal in Real-Time", Institute for Computer Science and Applied Mathematics Christian-Albrechts University of Kiel, Germany,2003.
- [11] Lu N., Wang J., "An Improved Motion Detection Method for Real-Time Surveillance"IAENG *International Journal of Computer Science*, 2008